EARTHQUAKE ENGINEERING AND STRUCTURAL DYNAMICS
Earthquake Engng. Struct. Dyn. **27**, 1331–1346 (1998)

PROBABILISTIC CONTROL FOR THE ACTIVE MASS DRIVER BENCHMARK STRUCTURAL MODEL

B. SCOTT MAY† AND JAMES L. BECK*,‡
Department of Civil Engineering, California Institute of Technology, Pasadena, CA 91125, U.S.A.

SUMMARY

A probability-based robust control design methodology is presented that is applied to the 'benchmark system', which is a high-fidelity model of an active-mass-driver laboratory structure. For the controller design, the objective is to maximize the probability that the uncertain structure/controller system achieves satisfactory performance when subject to uncertain excitation. The controller's robust performance is computed for a set of possible models by weighting the conditional performance probability for a particular model with the probability of that model, then integrating over the set of possible models. This is accomplished in an efficient manner using an asymptotic approximation. The probable performance is then maximized over the class of constant-gain acceleration-feedback controllers to find the optimal controller. This control design method is applied to a reduced-order model of the benchmark system to obtain four controllers, two that are designed on the basis of a 'nominal' system model and two 'robust' ones that consider model uncertainty. The performance is evaluated for the closed-loop systems that are subject to various excitations. © 1998 John Wiley & Sons, Ltd.

KEY WORDS: active mass driver; benchmark structure; structural control; robust control; probabilistic control

1. INTRODUCTION

A probabilistic methodology is used for the design of a robust controller for the 'benchmark system', which is a high-fidelity model of an active mass driver (AMD) laboratory structure that is described by Spencer *et al.*[1] This model is available from the World Wide Web at `http://www.nd.edu/~quake`. Using the total probability theorem,[2] the probability of satisfactory performance for a particular controller is obtained by integrating the performance of a particular model, weighted by that model's probability, over all possible models. The design objective for the controller is to maximize the probability of achieving satisfactory performance, or equivalently, to minimize the probability that the system fails to achieve satisfactory performance, henceforth termed the 'failure probability'. Satisfactory performance is achieved when the response variables of interest, in this case the benchmark system's interstorey drifts and the AMD actuator stroke and acceleration, remain within specified 'safe' levels over a given time period. In this study, the parameters describing the Kanai-Tajimi excitation model have the greatest uncertainty, and the parameters describing the reduced-order linear model of the benchmark system that is used for design purposes are assumed to be accurate. For this application, therefore, the controller is 'robust' with respect to a set of possible stochastic excitation models only, although the methodology can also include a set of possible structural models for the system.

* Correspondence to: James L. Beck, Department of Civil Engineering, California Institute of Technology, Pasadena, CA 91125, U.S.A.
E-mail: jimbeck@cco.caltech.edu
† Graduate Student
‡ Professor

Contract/grant sponsor: National Science Foundation; Contract/grant number: CMS-9503370

CCC 0098–8847/98/111331–16$17·50

Received 12 July 1997
Revised 2 December 1997

The probabilistic robust control approach creates controllers that incorporate probabilistic descriptions of the model uncertainties into the design of the optimal controller. The controllers are designed to satisfy probable performance over the class of uncertain models, and may be less conservative than those designed using methods based on the worst-case performance (e.g. $\mathscr{H}_\infty$-control and its derivatives), where the 'worst' model may be quite improbable. Probabilistic uncertainty descriptions can arise when models of the system are identified using response data, or when the modeling uncertainties in describing the system are quantified based on engineering experience.

Stengel and Ray[3] and Marrison and Stengel[4] have investigated control system analysis and synthesis for uncertain systems using Monte Carlo simulation methods. Spencer *et al.*,[5,6] Field *et al.*,[7,8] have investigated alternatives to Monte Carlo simulation for probabilistic control analysis and design using first- and second-order reliability methods (FORM/SORM) to compute the probable performance. In the methodology introduced in this work, an efficient asymptotic method[9] is used to approximate the probability integrals to determine the system's performance.

The next section of the paper describes the design methodology for the probabilistic robust controller. Section 3 summarizes the model description, uncertain variables, and probabilistic performance measures used for the AMD benchmark problem. Section 4 describes the four controllers that are designed for this problem using a nominal reduced-order linear model of the benchmark system. The first two controllers are designed using the Kanai-Tajimi filter parameters that are considered the 'most probable' under a probabilistic description of the input-model uncertainty. The other two controllers are designed to be robust with respect to the possible variations in the Kanai-Tajimi filter parameters. Results from the simulated responses of the closed-loop systems that incorporate these controllers are presented in Section 5.

2. PROBABILISTIC CONTROLLER DESIGN

2.1. Failure probability calculation

The design objective for the probabilistic robust controller is to minimize the failure probability of the composite structure–actuator system for a class of uncertain models that could represent the system and excitation. The total failure probability, as implied by the total probability theorem,[2] is given by integration over all the possible models of the probability of failure conditional on a particular model weighted by the probability assigned to that model.

Failure is defined to occur when at least one of the response quantities for a system model exists the 'safe' region for the first time. The safe region, denoted $\mathscr{S}$, is the region in performance-variable space bounded by the failure thresholds for the various failure possibilities. The failure region is the complement of this region, and is represented by $\mathscr{F}$. In the benchmark example, failure is defined to occur when the relative drift between adjacent storeys exceeds a certain level, or when the AMD actuator stroke or actuator acceleration exceed certain levels. The failure probability is denoted by

$$\mathscr{P}(\mathscr{F}\,|\,\theta,\phi) := \mathscr{P}[\sim\{x(t)\in\mathscr{S},\ \forall t\in(0,T]\}\,|\,\theta,\phi] \tag{1}$$

where $\sim$ denotes the logical 'not'. This failure probability is conditional on the particular model that is chosen to represent the system, where the particular model, θ, is a member of the set of possible models for the system, Θ, as well as the controller that is chosen for the system, $\phi\in\Phi$, where Φ represents the set of allowable controllers.

This failure probability calculation is the classic 'first-passage' problem, which has no known exact solution for a dynamic system subject to random excitation.[10] Hence, an approximate solution must be used. The approximation is based on threshold-crossing theory,[10] which estimates the mean rate that a random process crosses a specified boundary in the outward direction, and is termed the 'out-crossing rate'.

Calculation of the failure probability from the out-crossing rate involves treating the failures as independent arrivals of a Poisson process. Using the Poisson approximation, $\mathscr{P}(\mathscr{F}\,|\,\theta,\phi)$ is the probability of at least

one failure during the time interval $(0, T]$, assuming an unfailed system initially, so

$$\mathscr{P}(\mathscr{F}\,|\,\theta,\phi) \simeq 1 - \exp\left[-\int_0^T \nu_\beta(\theta,\phi,t)\,\mathrm{d}t \right] \tag{2}$$

where $\nu_\beta(\theta,\phi,t)$ is the mean out-crossing rate of the threshold level β. Additionally, under the assumption of stationarity, $\nu_\beta(\theta,\phi,t) = \nu_\beta(\theta,\phi)$ is independent of time, so the conditional failure probability is approximated by

$$\mathscr{P}(\mathscr{F}\,|\,\theta,\phi) \simeq 1 - \exp[\,-\nu_\beta(\theta,\phi)\,T\,] \tag{3}$$

For a scalar-valued Gaussian process where the random variable $X(t)$ and its derivative $\dot{X}(t)$ are independent and normally distributed, with means of zero and variances of σ_x and $\sigma_{\dot{x}}$, respectively, the number of outward crossings per unit time of the two-sided threshold $\pm\beta$ is[10]

$$\begin{aligned} \nu_\beta &= \int_{-\infty}^{\infty} \dot{x} f_{X\dot{X}}(\beta,\dot{x})\,\mathrm{d}\dot{x} \\ &= \frac{\sigma_{\dot{x}}}{\pi\sigma_x} \exp\left[-\frac{1}{2}\frac{\beta^2}{\sigma_x^2} \right] \end{aligned} \tag{4}$$

For vector processes, the out-crossing rate can be obtained by integrating the joint probability density function of the response, $f_{X\dot{X}}(x,\dot{x})$, evaluated at each failure surface, for all velocities with components pointing outward from that surface, then summing this quantity over all the failure surfaces. Unfortunately, when the response variables are correlated, this is often a difficult integration even for low-dimensional failure surfaces. For simplification, an upper bound on the composite failure probability is used, which is given by adding together the probabilities for each failure possibility.

2.2. *Model uncertainty description*

Probability distributions assigned to the set of possible models for the system are used to quantify the relative plausibility of each model, where the plausibility of a model is related to its ability to predict the future response of the system.[11] These probabilities are specified based on the modeller's present state of knowledge of the system, where the knowledge can be a combination of theoretical modelling, system identification using previous response data, and 'engineering judgment'.

In addition to the modelling uncertainty, the nature of the disturbance is uncertain as well. In order to simulate the response of the system to an earthquake, the uncertain excitation is described by a Kanai-Tajimi stochastic model, that is by a Gaussian white noise process passing through a linear second-order filter. The output from the filter mimics the stationary portion of the strong ground shaking from an earthquake. The filter's peak frequency, damping ratio, and input magnitude parameters are considered uncertain, and are prescribed by *a priori* probability distributions.

2.3. *Total failure probability*

The total probability of failure is obtained by synthesizing the methods of the two previous sections. Based on the total probability theorem, an integral of the failure probability for a particular model (from Section 2.1), weighted by the probability of that model (from Section 2.2), over the set of all possible models yields the total failure probability,

$$J(\phi,\Theta) := \mathscr{P}(\mathscr{F}\,|\,\phi,\Theta) = \int_\Theta \mathscr{P}(\mathscr{F}\,|\,\theta,\phi)\,p(\theta\,|\,\Theta)\,\mathrm{d}\theta \tag{5}$$

This probability is conditional on the class of possible models, Θ, with its corresponding probability distribution, and the particular controller used, $\phi \in \Phi$.

Because the dimension of the integral grows with the number of uncertain parameters, an efficient method must be chosen to approximate the integral. The method used herein is an asymptotic expansion about the region of the integrand with the greatest contribution to the probability integral.[9,12,13] The asymptotic approximation is based on Laplace's method[14] for integrals of the form

$$I = \int_{\Theta} e^{l(\theta)}\, d\theta, \tag{6}$$

and involves fitting a Gaussian-type surface to the 'design point', or maximum, of the integrand in equation (5). In this application, an $l(\theta)$ of the form

$$l(\theta) = \log f(\theta) + \log g(\theta) \tag{7}$$

can be chosen, where $f(\theta) := \mathscr{P}(\mathscr{F} \mid \theta, \phi)$ and $g(\theta) := p(\theta \mid \Theta)$, from equation (5). Then, the integral (5) can be approximated by

$$J(\phi, \Theta) \simeq (2\pi)^{n/2} \frac{h(\theta^*) g(\theta^*)}{\sqrt{\det L(\theta^*)}} \tag{8}$$

where θ^* maximizes equation (7) [and so the integrand of equation (5)], and $L(\theta^*)$ is the Hessian of $l(\theta)$ evaluated at θ^*. See Reference 9 for the details of this derivation. Since an optimization must be performed to find the design point for the asymptotic expansion, the computation time required for this technique has an upper bound that grows exponentially with the number of uncertain parameters. Monte Carlo integration is another alternative, where the number of computations required to obtain an estimate of the solution depends only on the desired accuracy and not the dimension of the integral. However, the Monte Carlo technique is expected to be prohibitively expensive computationally for the small failure probabilities that are desired for a structure.

2.4. Controller optimization

The optimization seeks the particular controller $\hat{\phi}$ out of the class of possible controllers Φ that minimizes the cost function of the total failure probability described above in equation (5), that is,

$$J(\hat{\phi}, \Theta) = \min_{\phi \in \Phi} J(\phi, \Theta) \tag{9}$$

Solution of equation (9) requires a nonlinear optimization that can be performed using a variety of existing numerical methods (see References 15 or 16, for example). The integration of equation (5) in the previous section must be performed for each function evaluation in the optimization, so in the worst case the solution time grows exponentially with both the number of uncertain parameters and the number of parameters in the control law. The optimization method that is used in this paper to find the design points for the asymptotic integration of equation (5) and to compute the controllers in equation (9) is an adaptation of the Nelder and Mead nonlinear simplex algorithm[16] that is implemented in MATLAB[17] as the function `fmins( )`. To illustrate the probabilistic control design methodology in the benchmark example, a simple controller class is chosen, which is the class of acceleration-feedback controllers, where a low-pass filter that serves as a frequency-dependent weighting function on the controller's performance is incorporated into the controller. This dynamic compensation proves necessary to reduce the sensitivity of the system to sensor noise and modeling error, as unfiltered high-frequency signals significantly increase the required actuator acceleration. In two separate controller designs for the system that are discussed further in Sections 4 and 5, the roll-off frequency for the low-pass filter is both selected *a priori* and allowed to vary as an additional controller parameter.

3. AMD BENCHMARK PROBLEM DEFINITION

3.1. Overview

The various facets of the probabilistic robust control methodology are illustrated by designing a controller for the AMD benchmark system.[1] The closed-loop system is a SIMULINK[18] model that is created by inter-connecting the controller with a high-fidelity evaluation model of a laboratory structure. The SIMULINK model incorporates many of the features of the actual laboratory system, such as actuator and sensor saturation, sensor noise, time delays, and discretization errors. The system response is obtained through numerical integration of the equations of motion represented in the SIMULINK model. To reduce integration errors, the integration is performed for a time-step of 0·0001 sec, while the inputs and the controller are updated every 0·001 sec. The system's performance with the probabilistic robust controller is obtained for a variety of performance measures, so the controller can then be compared with controllers synthesized for the same test-bed using other methods.

3.2. System description

The benchmark system is based on a high-fidelity 28-state linear model of a laboratory structure, which captures the structure's behaviour in the frequency range from 0 to 100 Hz. The inputs to this linear model are the ground acceleration, $\ddot{x}_g$, the control force, u, and the sensor noise, v. The outputs are the measured outputs,

$$y = \{x_m \;\; \ddot{x}_{a1} \;\; \ddot{x}_{a2} \;\; \ddot{x}_{a3} \;\; \ddot{x}_{am} \;\; \ddot{x}_g\}',$$

which are the potential controller inputs, and the vector of performance variables,

$$z = \{x_1 \;\; x_2 \;\; x_3 \;\; x_m \;\; \dot{x}_1 \;\; \dot{x}_2 \;\; \dot{x}_3 \;\; \dot{x}_m \;\; \ddot{x}_{a1} \;\; \ddot{x}_{a2} \;\; \ddot{x}_{a3} \;\; \ddot{x}_{am}\}'.$$

The quantities x_1, x_2, x_3, and x_m represent the displacement of the structure at floors 1, 2, and 3, and the actuator displacement, respectively; $\dot{x}_1$, $\dot{x}_2$, $\dot{x}_3$ and $\dot{x}_m$ are the velocities at these locations; and $\ddot{x}_{a1}$, $\ddot{x}_{a2}$, $\ddot{x}_{a3}$, $\ddot{x}_{am}$ are the absolute accelerations. The state-space model for this 28-state 'evaluation' model is distributed with the benchmark SIMULINK model.

As specified by Spencer *et al.*,[1] the measurement noise is modelled by a Gaussian distribution with zero mean and standard deviation of $v_{rms} = 0{\cdot}01$ V. This signal is implemented in the SIMULINK model as a discrete Gaussian process calculated at each $\Delta T = 0{\cdot}001$ sec, and is held constant for the integration over the duration of that interval. This noise is added to each measured output channel in the simulation.

3.3. Design model description

A linear 10-state reduced-order 'design' model of the benchmark system is provided for controller design purposes.[1] The reduced-order model closely tracks the behaviour of the 28-state linear model in the frequency range from 0 to 30 Hz. This frequency range includes the three fundamental structural modes that are the primary contributors to the inter-storey drifts. The system matrices A_r, B_r, E_r, C_{yr}, C_{zr}, D_{yr}, D_{zr}, F_{yr}, and F_{zr} associated with the reduced-order system are also distributed with the SIMULINK benchmark model. The state-space equations of motion for this reduced-order model are given by

$$\begin{aligned} \dot{x} &= A_r x + [B_r \;\; E_r \;\; 0] \begin{Bmatrix} u \\ \ddot{x}_g \\ v_r \end{Bmatrix} \\ \begin{Bmatrix} y \\ z \end{Bmatrix} &= \begin{bmatrix} C_{yr} \\ C_{zr} \end{bmatrix} x + \begin{bmatrix} D_{yr} & F_{yr} & \sigma_r I_y \\ D_{zr} & F_{zr} & 0 \end{bmatrix} \begin{Bmatrix} u \\ \ddot{x}_g \\ v_r \end{Bmatrix} \end{aligned} \tag{10}$$

The 'noise', v_r, in equation (10) includes both the sensor noise and the model error, which is the error between the output from the benchmark system and the output predicted by the reduced-order model. Hence, v_r is scaled by σ_r, where $\sigma_r \geqslant 0{\cdot}01$ V, such that the noise term has the appropriate standard deviation, and v_r is modelled as a zero-mean and unit-variant Gaussian process.

The performance variables included in the design objective are the inter-storey drifts and the relative position and absolute acceleration of the actuator. Denote the variables needed to compute the failure probabilities for these performance variables by

$$z_p := \{d_1 \;\; d_2 \;\; d_3 \;\; x_m \;\; \dot{d}_1 \;\; \dot{d}_2 \;\; \dot{d}_3 \;\; \dot{x}_m \;\; \ddot{x}_{am} \;\; \tilde{\dot{x}}_{am}\}'$$

where $d_i := (x_i - x_{i-1})$ is the interstorey drift for storey i, $\dot{d}_i$ is its velocity, and x_m, $\dot{x}_m$, and $\ddot{x}_{am}$ are the position, velocity, and acceleration of the actuator mass, respectively. The quantity $\tilde{\dot{x}}_{am}$ is an estimate of the derivative of the actuator's acceleration, which is required for the failure probability calculation in equations (3) and (4), and is obtained using a filter that mimics a differentiator at frequencies below 30 Hz. The differentiator's transfer function is given by

$$H_{\tilde{\dot{x}}_{am}\ddot{x}_{am}} = \frac{\omega_{af}^2 s}{s^2 + 2\zeta_{af}\omega_{af} s + \omega_{af}^2}, \tag{11}$$

with $\omega_{af} = 188{\cdot}5$ rad/sec and $\zeta_{af} = 1/\sqrt{2}$. Let the system G_z denote the relationship between z and z_p such that $z_p := G_z z$.

In addition, the control law is constructed using the acceleration feedback from the accelerometers mounted on each floor, which is a subset of the entire output vector y. Hence, $y_c = L_y y$, where $y_c = \{\ddot{x}_{a1}\, \ddot{x}_{a2}\, \ddot{x}_{a3}\}'$.

The controller objective is evaluated on the basis of the theoretical stationary system response to a filtered white-noise excitation, where the filter is the well-known Kanai–Tajimi filter,[19] such that the spectrum of the filter output mimics that of the stationary portion of a 'typical' earthquake. The power spectral density function for this filter is

$$S_{\ddot{x}_g\ddot{x}_g}(\omega) = \frac{S_0(4\zeta_g^2\omega_g^2\omega^2 + \omega_g^4)}{(\omega^2 - \omega_g^2)^2 + 4\zeta_g^2\omega_g^2\omega^2} \tag{12}$$

which can be represented in the time domain with the following state equations:

$$\begin{aligned} \dot{x}_f &= A_f x_f + B_f w \\ \ddot{x}_g &= C_f x_f \end{aligned} \tag{13}$$

where w is zero-mean Gaussian white noise with unit intensity,

$$A_f := \begin{bmatrix} 0 & 1 \\ -\omega_g^2 & -2\zeta_g\omega_g \end{bmatrix}, \quad B_f := \begin{bmatrix} 0 \\ 1 \end{bmatrix},$$

and

$$C_f := \sqrt{S_0 2\pi}\,[\omega_g^2 \;\; 2\zeta_g\omega_g].$$

Also, S_0 is specified by Spencer *et al.*[1] such that the input variance is uniform for all ω_g and ζ_g, so

$$S_0 := \sigma_w^2 \frac{0{\cdot}03\zeta_g}{\omega_g(4\zeta_g^2 + 1)}\, \mathrm{g}^2\,\mathrm{sec}. \tag{14}$$

The constant σ_w is used to scale the input variance for different levels of excitation, and $\sigma_w = 1$ implies $\sigma_{\ddot{x}_g} = 0{\cdot}12g$.

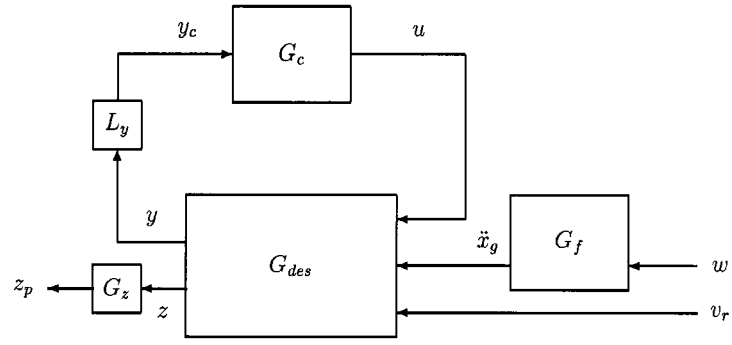

Figure 1. Closed-loop interconnection for controller design

Define G_m to represent a general linear system given by the state-space equations of motion $\dot{x} = A_m x + B_m w$, $y = C_m x + D_m w$. Using this notation, let G_{des} represent the state equations (10) for the linear 'design' model, G_{f} the Kanai–Tajimi filter of equation (13), and G_{c} the state equations for the controller. A block diagram of the system interconnection for this design model of the benchmark system is shown in Figure 1.

3.4. *Model uncertainty*

Uncertainty exists in the model parameters for the Kanai–Tajimi filter, ω_{g}, ζ_{g}, and the input variance, σ_{w}, which scales S_0 in equation (14). The parameters describing the design model of the benchmark system are assumed to be sufficiently accurate to be considered 'certain' for estimating the response in the frequency range of interest. The probability density functions (PDFs) chosen to model the uncertain input parameters are shown in Figure 2, and are described as follows:

1. ω_{g} is log-normally distributed with mean 50 rad/sec and $\sigma_{\log \omega_{\mathrm{g}}}$, = 0·2,
2. ζ_{g} is log-normally distributed with mean 0·5 and $\sigma_{\log \zeta_{\mathrm{g}}}$, = 0·2, and
3. σ_{w} is log-normally distributed with mean 1·0 and $\sigma_{\log \sigma_{\mathrm{w}}}$, = 0·2.

The choice of these particular PDFs to model the uncertainty is somewhat arbitrary. However, the total failure probability does not depend strongly on the form of the probability models, because the value of the integral in equation (5) is determined largely by the integrand's behaviour at its peak, provided the choices for the probability models have the same most-probable values and similar shapes to their distributions about that point. So, although other probability models could be considered for the parametric uncertainty, such as the normal distribution or the χ^2 distribution, their PDFs would appear similar in the region of greatest contribution to equation (5), and hence would yield nearly identical probabilistic performance levels.

Spencer *et al.*[1] specify a range of uncertainty for ω_{g} and ζ_{g}, given by 20 rad/sec $\leqslant \omega_{\mathrm{g}} \leqslant$ 120 rad/sec and $0{\cdot}30 \leqslant \zeta_{\mathrm{g}} \leqslant 0{\cdot}75$, which is reflected in the PDFs that are used. In addition, σ_{w} is allowed to vary to represent the uncertainty in the earthquake intensity. For example, for the two earthquake records provided, σ_{w} is 1·4 for the El Centro record and 1·2 for the Hachinohe record, where the variance is calculated using the entire duration of the records. In practice, with a careful study of soil conditions of a structure, its proximity to major faults, and other factors, the PDFs for these ground-motion parameters could be modified appropriately to reflect the local site conditions. The variables are assumed to be stochastically independent, so the joint PDF is the product of these PDFs.

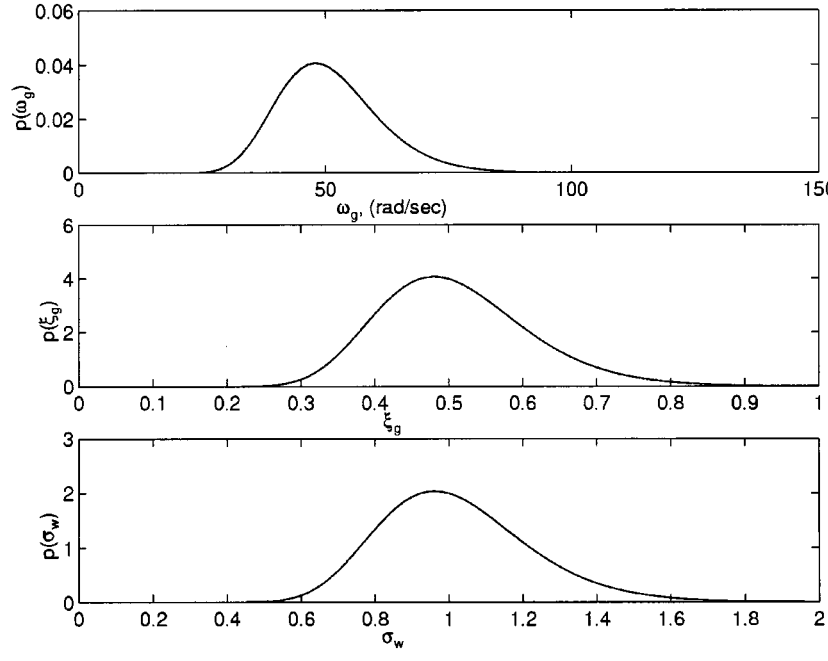

Figure 2. Probability density functions for the uncertain variables ω_g, ζ_g, and σ_w

3.5. *Performance measures*

While the probabilistic controllers are designed to minimize the failure probability of the closed-loop systems, in order to compare this design with other control methodologies, its 'performance' is assessed using the ten evaluation criteria proposed by Spencer *et al.*,[1] which represent measures of a variety of response quantities. Evaluation criteria J_1 through J_5 represent root-mean-square (RMS) response quantities for the controlled system. These quantities are normalized by the RMS response of the uncontrolled system for the 'worst-case' Kanai–Tajimi filter parameters ω_g and ζ_g with $\sigma_w = 1$, where 'worst' is defined in terms of the peak RMS system response over the range of possible ω_g and ζ_g. These response ratios are the maximum RMS interstorey drift over all stories (J_1), the maximum RMS absolute acceleration over all floors (J_2), the RMS actuator displacement relative to the third storey (J_3), the RMS relative actuator velocity (J_4), and the RMS absolute actuator acceleration (J_5). The quantities J_1 and J_3 are normalized by the RMS relative displacement of the third floor with respect to the base for the uncontrolled system with $\omega_g = 37{\cdot}3$ rad/sec, $\zeta_g = 0{\cdot}3$, $\sigma_w = 1$, where the RMS displacement is $\sigma_{x_{3}0} = 1{\cdot}31$ cm. Criterion J_4 is normalized by the third floor RMS relative velocity, $\sigma_{\dot{x}_{3}0} = 47{\cdot}9$ cm/sec, and J_2 and J_5 are normalized by the RMS absolute acceleration of the third floor, $\sigma_{\ddot{x}_{a30}} = 1{\cdot}79$ g. The RMS response quantities for the controlled system are obtained via a SIMULINK[18] simulation by averaging the response to 300 sec of computer-generated random noise.

Evaluation criteria J_6 through J_{10} represent the peak values of the same response quantities for the deterministic response of the closed-loop system to two scaled earthquake inputs, the north–south component of the 1940 El Centro earthquake, and the north–south component of the 1968 Hachinohe earthquake. These criteria are normalized by the peak response quantities of the uncontrolled system for each earthquake. For the El Centro response, J_6 and J_8 are normalized by $x_{30} = 3{\cdot}37$ cm, J_9 by $\dot{x}_{30} = 131$ cm/sec, and J_7 and J_{10} by $\ddot{x}_{a30} = 5{\cdot}05$ g. For the Hachinohe response, J_6 and J_8 are normalized by $x_{30} = 1{\cdot}66$ cm, J_9 by $\dot{x}_{30} = 58{\cdot}3$ cm/sec, and J_7 and J_{10} by $\ddot{x}_{a30} = 2{\cdot}58g$.

4. CONTROLLER DESIGN

4.1. Controller class

The following state equations are used to describe the linear control system G_c:

$$\dot{x}_c = A_c x_c + B_c y_c$$
$$u = C_c x_c \tag{15}$$

where x_c contains the states of a low-pass filter and B_c contains the output-feedback gains.

Output-feedback controllers are chosen for the control design optimization, where the measured absolute acceleration of each floor of the benchmark system is fed back to the controller. Since the primary contribution to the inter-storey drift for earthquake excitations is expected to come from the flexible modes of the structure, which all occur below 30 Hz for the uncontrolled system, a frequency-dependent weighting function is included in the controller that seeks to minimize the structural response in this lower-frequency range and to reduce the control effort in the range of the higher-frequency noise and modelling error. The roll-off frequency for the low-pass weighting function, when specified *a priori* rather than included in a controller design, is $\omega_b = 30$ Hz $= 188{\cdot}5$ rad/sec, and the low-pass filter is a second-order Butterworth filter. Therefore, the controller has a state of dimension 2, and easily satisfies the controller dimension limit of 12 specified for the benchmark problem.[1] The controller parameters that are free to be chosen are the three proportional-feedback gains, $K = \{k_1 \;\; k_2 \;\; k_3\}$, that multiply the accelerations from the sensors at floors 1, 2, and 3 of the benchmark system, respectively, and sometimes ω_b, when this is allowed by vary as a design parameter.

Four controllers are designed for the AMD benchmark model. The first two, termed the 'nominal-model controllers', are designed using the reduced order 'design' model to minimize the failure probability for a particular Kanai–Tajimi excitation model. This model uses the parameter values $\omega_g = 50{\cdot}0$ rad/sec, $\zeta_g = 0{\cdot}5$, and $\sigma_w = 1$, which correspond to the mean parameters probabilities (and are close to the most probable ones) for the PDFs given in Figure 2. The second two controllers, termed the 'uncertain-model controllers', are again designed using the reduced-order design model to minimize the total failure probability. These controllers explicitly incorporate the probability models for the uncertainty of the excitation model parameters ω_g, ζ_g, and σ_w, which were described earlier. The initial guess during the optimization for the uncertain-model control-feedback gains is taken from the result from the nominal-model controller optimization. For each case (nominal model and uncertain model), one controller is designed for the three output-feedback gains using a roll-off frequency of $\omega_b = 30$ Hz $= 188{\cdot}5$ rad/sec for the low-pass filter. The other controllers include this roll-off frequency as a design parameter for the controller optimization.

Note that direct output-feedback without a dynamic compensator was originally considered by the authors. However, satisfactory performance was not attainable in this case, because the actuator acceleration is too large due to the higher-frequency sensor noise and modeling error. A study of the affect of the roll-off frequency for the low-pass filter on the performance was also conducted, and lower roll-off frequencies were observed to reduce the acceleration requirements for the AMD actuator that constrain the probabilistic performance. Concurrently, the AMD displacements increase, but they do not begin to constrain the performance until the normalized AMD acceleration and displacement levels are comparable.

4.2. Failure probability calculation

As shown in equation (4), the out-crossing rate of a scalar stochastic process is simply a function of the variance of the response and its derivative. The variances of the response quantities are obtained by solving the Lyapunov equation associated with the closed-loop system pictured in Figure 1. These are substituted into equation (4), then the approximate failure probability for each model is obtained from equation (3). For the 'uncertain-model' controller, the total failure probability given by equation (5) is then evaluated using the asymptotic expression[9] from equation (8).

Let G_{clp}, with inputs w and v and output z_{p}, be the system formed by the closed-loop inter-connection of Figure 1, so G_{clp} has the following form, where the system matrices can be derived from equation (10), (13), and (15):

$$\begin{aligned} \dot{x}_{\text{clp}} &= A_{\text{clp}} x_{\text{clp}} + B_{\text{clp}} \begin{Bmatrix} w \\ v \end{Bmatrix} \\ z_{\text{p}} &= C_{\text{clp}} x_{\text{clp}}, \end{aligned} \tag{16}$$

where $x_{\text{clp}} = \{x_{\text{c}}' \, x' \, x_{\text{f}}'\}'$ represents the state of the closed-loop system, and z_{p} is its output. The covariance matrix of the performance variables is as follows:

$$E[z_{\text{p}} z_{\text{p}}'] = C_{\text{clp}} R C_{\text{clp}}', \tag{17}$$

where 'E' denotes expected value, and

$$R := E[x_{\text{clp}} x_{\text{clp}}'] \tag{18}$$

is the solution to the standard Lyapunov equation

$$A_{\text{clp}} R + R A_{\text{clp}}' + B_{\text{clp}} B_{\text{clp}}' = 0 \tag{19}$$

The failure possibilities considered for this example include the interstorey drifts, and 'failure' occurs when the drift in any one storey exceeds the drift limit β, where the limit is chosen to be 1·5 cm, or approximately 3 per cent of the storey height in the laboratory structure. In practice, assuming the purpose of the structural control system is to ensure the safety of a structure and its occupants, the limiting value for the inter-storey drift should correspond to the displacement level which would cause structural damage, and attaining a drift ratio of 3 per cent during an earthquake would typically imply some damage has occurred in a moment-resisting steel frame (similar to the laboratory structure). Additional failure possibilities for the AMD benchmark model are that the actuator exceeds the limits of its stroke and its maximum allowable acceleration. Hence, for the AMD actuator, failure is defined to occur when the required actuator displacement, x_m, exceeds its stroke of $\pm \xi_1 = 9$ cm, or when the required actuator acceleration, $\ddot{x}_{am}$, exceeds $\pm \xi_2 = 6g$.

Other failure possibilities could be considered for control design of a structure, such as exceeding the maximum allowable base shear force, exceeding comfortable acceleration levels in the structure, or for the actuator, exceeding the actuator power or force limits. The control objective can easily be re-defined to represent a different combination of these possible failures.

An illustration of a three-dimensional projection of the failure surface is shown in Figure 3 (note that the true failure surface is five-dimensional for this problem). The three dimensions pictured are the drifts for the first two stories (d_1 and d_2), and the actuator displacement (x_m). The complete 'safe' region is defined by

$$\mathscr{S} := \left\{ \begin{matrix} \max(|d_1(t)|, \; |d_2(t)|, \; |d_3(t)|) \leqslant \beta \\ |x_m(t)| \leqslant \xi_1, \; |\ddot{x}_{am}| \leqslant \xi_2 \end{matrix} \quad \text{for } t \in (0, T] \right\} \tag{20}$$

where $T = 10$ sec. The failure surface boundary, $\partial\mathscr{S}$, is defined by $\beta = 1{\cdot}5$ cm, $\xi_1 = 9$ cm, and $\xi_2 = 6g$.

5. RESULTS

5.1. Nominal-model controllers

Controller 1, the nominal-model controller designed using $\omega_{\text{b}} = 188{\cdot}5$ rad/sec and gound-motion parameters $\omega_{\text{g}} = 50$ rad/sec, $\zeta_{\text{g}} = 0{\cdot}50$, has the acceleration feedback gains $K_1 = \{0{\cdot}0339 \;\; 0{\cdot}0538 \;\; 0{\cdot}0958\}$ (see Table I for a summary of the various controller designs). The ten performance criteria J_1–J_{10} are listed for this model in Table II. The criteria J_1–J_5 are evaluated by simulating the response of the closed-loop system

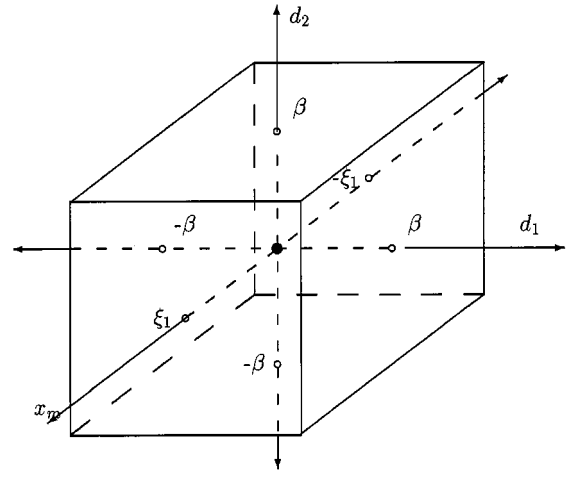

Figure 3. Safe region in response-variable space

Table I. Controller parameters used for performance evaluations

Name	ω_b (rad/sec)	k_1	k_2	k_2
Controller 1	188·5	0·0339	0·0538	0·0958
Controller 2	33·4	0.354	0.320	0.237
Controller 3	188·5	0·0454	0·0576	0·126
Controller 4	33·1	0·431	0·291	0·235

in SIMULINK to a stationary computer-generated 'white' signal with variance $\sigma_{\ddot{x}_g} = 0{\cdot}12g$, with the nominal Kanai–Tajimi filter parameters $\omega_g = 37{\cdot}3$ rad/sec and $\zeta_g = 0{\cdot}3$, for 300 sec duration, then computing the variances of the relevant response variables. These quantities J_1–J_5 are not maximized over the Kanai–Tajimi filter parameters ω_g and ζ_g, as this proves to be too computationally expensive for the resources available to the authors.

For Controller 2, ω_b is allowed to vary as a controller design parameter, and the gains $K_2 = \{0{\cdot}354\ \ 0{\cdot}320\ \ 0{\cdot}237\}$ are found along with $\omega_b = 33{\cdot}4$ rad/sec. Note from Table II that this controller has significantly better performance than Controller 1. The simulated response of the closed loop system formed using Controller 2 to the scaled NS component of the 1940 El Centro earthquake is displayed in Figure 4, and to the NS component of the 1968 Hachinohe earthquake in Figure 5. For comparison, the El Centro record, as well as the response of the uncontrolled system to that input, are shown in Figure 6. The Fourier amplitude spectra of the first-storey drift response of both the controlled and uncontrolled system when subject to the El Centro input are shown in Figure 7, where the attenuation of the first two modes of vibration by the controller action is apparent.

The controller is successful in reducing the inter-storey drifts, as the maximum drift calculated for the controlled system during the El Centro earth-quake is 1·17 cm (compared to 2·09 cm for the uncontrolled system), and only 0·631 cm of drift is achieved during the Hachinohe earthquake (versus 0·958 cm for the uncontrolled system). The maximum actuator displacements which are found for these inputs are 4·46 and 2·69 cm, and the maximum accelerations are 4·22 and $2{\cdot}39g$. For the earthquake inputs, the maximum

Table II. Controller performance under various evaluation criteria

		Controller number			
		Nominal		Robust	
	Performance measure	1 Fixed ω_b	2 Optimal ω_b	3 Fixed ω_b	4 Optimal ω_b
Mean Square response	J_1	0·314	0·208	0·292	0·207
	J_2	0·510	0·345	0·473	0·345
	J_3	0·601	0·841	0·664	0·851
	J_4	0·598	0·823	0·659	0·832
	J_5	0·967	0·676	0·996	0·683
	$\|\| x_m(t) \|\|_2$ (cm)	0·79	1·10	0·87	1·11
	$\|\| \ddot{x}_{am}(t) \|\|_2$ (g)	1·73	1·21	1·78	1·22
	$\|\| u(t) \|\|_2$ (V)	0·15	0·29	0·18	0·30
Maximum El Centro response	J_6	0·423	0·347	0·401	0·345
	J_7	0·687	0·536	0·671	0·535
	J_8	0·659	1·324	0·772	1·341
	J_9	0·634	1·186	0·722	1·200
	J_{10}	1·239	0·836	1·298	0·859
	$\|\| x_m(t) \|\|_\infty$ (cm)	2·22	4·46	2·60	4·52
	$\|\| \ddot{x}_{am}(t) \|\|_\infty$ (g)	6·26	4·22	6·56	4·34
	$\|\| u(t) \|\|_\infty$ (V)	0·51	1·25	0·62	1·26
Maximum Hachinohe response	J_6	0·483	0·380	0·467	0·380
	J_7	0·785	0·687	0·733	0·684
	J_8	0·729	1·618	0·858	1·644
	J_9	0·755	1·524	0·895	1·558
	J_{10}	1·225	0·928	1·308	0·936
	$\|\| x_m(t) \|\|_\infty$ (cm)	1·21	2·69	1·42	2·73
	$\|\| \ddot{x}_{am}(t) \|\|_\infty$ (g)	3·16	2·39	3·37	2·41
	$\|\| u(t) \|\|_\infty$ (V)	0·31	0·75	0·36	0·76
	P_f	20·2%	0·082%	18·5%	0·081%

response ratios J_6–J_{10} given in Table II occur during the Hachinohe earthquake. The maximum actuator displacements, accelerations, and input voltages, as well as the RMS values of these quantities, all satisfy the constraints for the AMD benchmark actuator[1] for Controller 2 (note that the maximum actuator acceleration of $6g$ is exceeded for Controller 1).

5.2. *Uncertain-model controllers*

Controllers 3 and 4 are designed for the uncertain model to explicitly provide robustness to parameter variations in the excitation model, where the PDFs for the uncertain variables are shown in Figure 2. Given a particular controller, the total failure probability is obtained through an asymptotic approximation to equation (5). This result is minimized over the space of acceleration output-feedback controller parameters, with $\omega_b = 188{\cdot}5$ rad/sec for Controller 3 while ω_b is free to vary for Controller 4.

The feedback gains for Controller 3 are $K_3 = \{0{\cdot}0454 \;\; 0{\cdot}0576 \;\; 0{\cdot}126\}$ and for Controller 4, with $\omega_b = 33{\cdot}1$, $K_4 = \{0{\cdot}431 \;\; 0{\cdot}291 \;\; 0{\cdot}235\}$. The ten performance criteria J_1–J_{10} are again shown in Table II. The response of

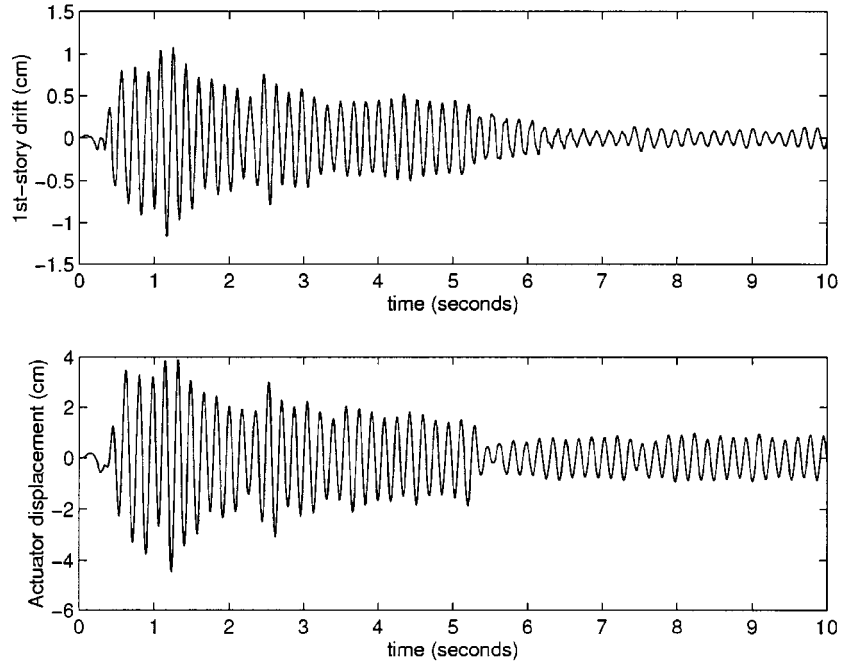

Figure 4. Structural response using Controller 2 to the El Centro earthquake

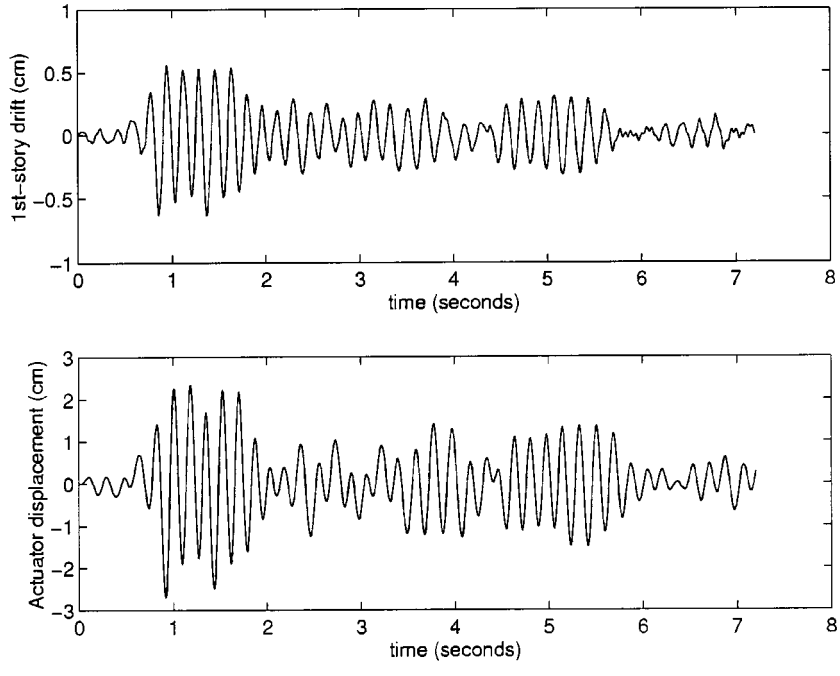

Figure 5. Structural response using Controller 2 to the Hachinohe earthquake

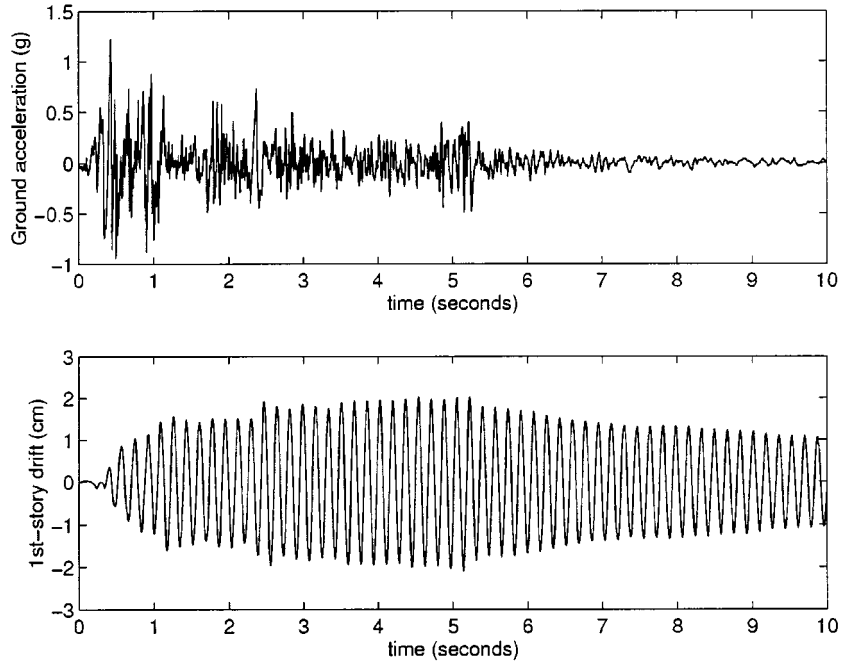

Figure 6. Scaled El Centro Earthquake excitation; response of the uncontrolled AMD model

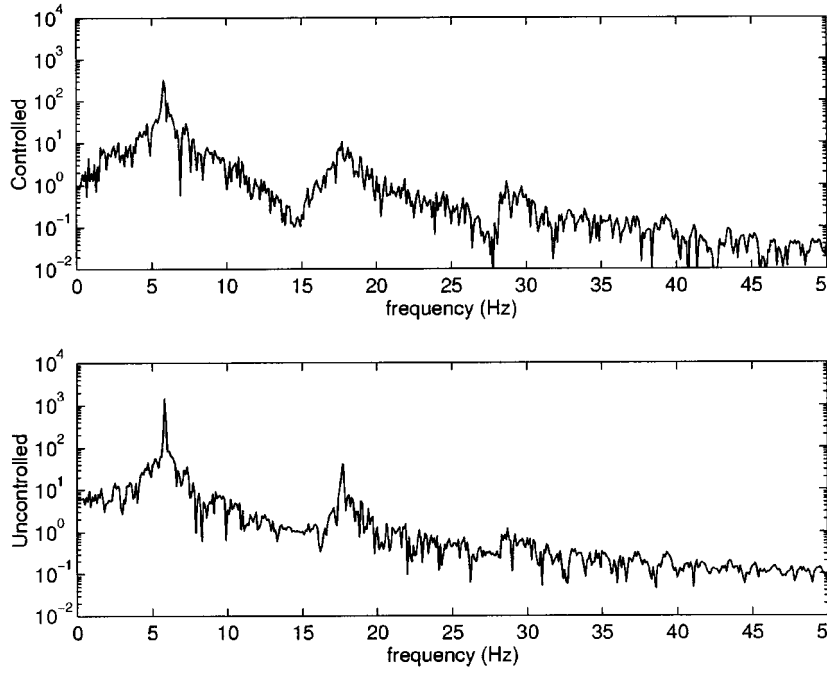

Figure 7. Fourier amplitude spectrum of the first-storey drift, controlled (with Controller 2) and uncontrolled systems, El Centro earthquake input

the closed-loop system for Controller 4 appears quite similar to that shown in Figures 4 and 5, so it is not repeated here. Again, the maximum actuator displacements, accelerations, and input voltages, as well as the RMS values of these quantities, all satisfy the constraints for the AMD benchmark actuator[1] for Controller 4, but the maximum actuator acceleration is exceeded for Controller 3.

The total failure probabilities can be calculated for both the uncertain model controllers and the nominal model controllers using the PDFs for the parametric uncertainty shown in Figure 2 and modelling the input as a (filtered) stationary white-noise process. The duration of the time interval for the failure probability calculation is taken to be 10 sec, yielding a failure probability of $P_{f1} = 20{\cdot}2\%$ for Controller 1, $P_{f2} = 0{\cdot}082\%$ for Controller 2, $P_{f3} = 18{\cdot}5\%$ for Controller 3, and $P_{f4} = 0{\cdot}081\%$ for Controller 4 compared to $P_{\text{func}} = 75{\cdot}2\%$ for the uncontrolled system (recall these are likely to be over-estimates of the 'true' failure probabilities, as they are upper bounds given by the sum of the failure probabilities for each failure possibility).

6. CONCLUSIONS

A consistent application of probability theory to the control of uncertain systems leads to the probabilistic robust control methodology outlined herein. Both the uncertainty in modeling the physical system as well as a reliability-based performance objective can be incorporated into the robust controller design.

The controllers that are designed for the AMD benchmark model achieve significant reductions in the failure probability of the controlled systems relative to the uncontrolled one, where the failure probability is found from the inter-storey drifts and the AMD actuator stroke and acceleration for this example. The benchmark controller constraints on the actuator command signal, acceleration, and displacement are satisfied for the two 'good' controllers and nearly for the other two.

One comment on the possible controller class for the system is that any parameterized controller could be considered for the problem, such as an output-feedback controller with a state estimator or a nonlinear controller. The only limit on the controller class is the efficiency of the optimization algorithm and the speed of the computer. A more complicated controller class, such as one containing a state estimator, might be expected to improve performance. This is a topic for further research.

A shortcoming of the approach that is presented is that the computation time required to solve the control design problem is significant for the uncertain-model controller (i.e., 1–2 h of CPU time for the controller designs presented previously, running MATLAB on a DEC/Alpha 3000 Work-station). While this is not a problem during the actual implementation of the controller, as the controller design is performed 'off line', it does slow down the controller design process. Another area for further research is to explore whether alternative probability-based performance objectives and uncertainty descriptions can be found that would lead to more efficient solution algorithms. Also, as experience is gained with this probabilistic analysis approach, more efficient computational procedures that can exploit the structure of a particular problem are likely to be developed.

ACKNOWLEDGEMENT

This paper is based upon work supported by the National Science Foundation under subcontract to grant CMS-9503370. This support is gratefully acknowledged.

REFERENCES

1. B. F. Spencer Jr., S. J. Dyke and H. S. Deoskar, 'Benchmark problems in structural control: Part I—Active mass driver system', *Earthquake Engng. Struct. Dyn.* **27**(11), 1127–1139 (1998).
2. A. Papoulis, *Probability, Random Variables, and Stochastic Processes*, McGraw-Hill, Inc., New York, 1965.
3. R. F. Stengel and L. R. Ray, 'Stochastic robustness of linear time-invariant control systems', *IEEE Trans. Automat. Control* **36**, 82–87 (1991).

4. C. I. Marrison and R. F. Stengel, 'Stochastic robustness synthesis applied to a benchmark control problem', *Int. J. Robust Nonlinear Control*, **5**, 13–31 (1995).
5. B. F. Spencer, Jr. and D. C. Kaspari, Jr., 'Structural control design: a reliability-based approach', *Proc. Amer. Control Conf.*, Baltimore, MD, 1994, pp. 1062–1066.
6. B. F. Spencer, Jr. and D. C. Kaspari, Jr., 'Reliability based optimal structural control', *Proc. 5th U.S. National Conf. on Earthquake Engineering*, 1994, pp. 703–712.
7. R. V. Field, Jr., W. B. Hall and L. A. Bergman, 'A MATLAB-based approach to the computation of probabilistic stability measures for controlled systems', *Proc. First World Conf. on Structural Control*, Pasadena, CA, 1994, pp. TP4-13-TP4-22.
8. R. V. Field, Jr., L. A. Bergman and W. B. Hall, 'Computation of probabilistic stability measures for a controlled distributed parameter system', *Probab. Engng. Mech.* **10**, 181–192 (1995).
9. C. Papadimitriou, J. L. Beck and L. Katafygiotis, 'Asymptotic expansions for reliabilities and moments of uncertain dynamic systems', *ASCE J. Engng. Mech.* **123**, 1219–1229 (1997).
10. Y. K. Lin, *Probabilistic Theory of Structural Dynamics*, Robert E. Krieger Publishing Company, Malabar, FL, 1976.
11. J. L. Beck, 'System identification methods applied to measured seismic response', *Proc. 11th World Conf. on Earthquake Engineering*, Acapulco, Mexico, 1996.
12. K. W. Breitung, 'Probability approximations by log likelihood maximization', *J. Engng. Mech. Div.* **117**, 457–477 (1991).
13. K. W. Breitung, 'Asymptotic approximations for probability integrals', *Probab. Engng. Mech.* **4**, 187–190 (1989).
14. K. W. Breitung, *Asymptotic Approximations for Probability Integrals*, Springer, Berlin, 1994.
15. D. A. Pierre, *Optimization Theory With Applications*, Dover, Mineola, NY, 1986.
16. W. H. Press, S. A. Teukolsky, W. T. Vetterling and B. P. Flannery, in *Numerical Recipes in C, the Art of Scientific Computing*, 2nd edn, Cambridge University Press, Cambridge, 1992.
17. *Matlab User's Guide*, The MathWorks, Inc., Natick, MA, 1994.
18. *Simulink User's Guide*, The MathWorks, Inc., Natick, MA, 1994.
19. R. W. Clough and J. Penzien, *Dynamics of Structures*, McGraw-Hill, Inc., New York, 1975.

